Drivers and surface signal of inter-annual variability of boreal stratospheric final warmings

Rémi Thiéblemont[1], Blanca Ayarzagüena[2,3], Katja Matthes[4,5], Slimane Bekki[6], Janna Abalichin[7] and Ulrike Langematz[7]

[1]Laboratoire des Sciences du Climat et de l'Environnement (LSCE), CNRS, Saint-Aubin, France.

[2]Universidad Complutense de Madrid (UCM), Madrid, Spain.

[3] Instituto de Geociencias, CSIC-UCM, Madrid, Spain.

[4]GEOMAR-Helmholtz Centre for Ocean Research, Kiel, Germany

[5]Christian-Albrechts-Universität zu Kiel (CAU), Kiel, Germany.

[6]Laboratoire Atmosphères, Milieux, Observations Spatiales (LATMOS), CNRS, Guyancourt, France.

[7]Freie Universität Berlin (FUB), Berlin, Germany.

Corresponding author: Rémi Thiéblemont (remi.thieblemont@latmos.ipsl.fr)

Abstract

Springtime stratospheric final warming (SFW) variability has been suggested to relate with the tropospheric circulation, particularly over the North Atlantic sector. These findings, however, are based on stratospheric reanalysis data that cover a rather short period of time (1979-present). The present work aims to improve the understanding of drivers, trends and surface impact of dynamical variability of boreal SFWs using a chemistry-climate model. We use multi-decadal integrations of the fully coupled chemistry-climate model CESM1(WACCM). Four sensitivity experiments are analyzed to assess the impact of external factors; namely the quasi-biennial oscillation (QBO), sea surface temperature (SST) variability and anthropogenic emissions. SFWs are classified into two types with respect to their vertical development; i.e. events may occur first in the mid-stratosphere (10-hPa first SFWs) or in the upper stratosphere (1-hPa first SFWs). Our results confirm previous reanalysis results regarding the differences in the time evolution of stratospheric conditions and near-surface circulation between 10-hPa and 1-hPa first SFWs. Additionally, a tripolar SST pattern is, for the first time, identified over the North Atlantic in spring months related to the SFW variability. Our analysis of the influence of remote modulators on SFWs revealed that the occurrence of major warmings in the previous winter favors the occurrence of 10-hPa first SFWs later on. We further found that QBO and SST variability significantly affect the ratio between 1-hPa first and 10-hPa first SFWs. Finally, our results suggest that ozone recovery may impact the timing of the occurrence of 1-hPa first SFWs.

1. Introduction

The stratospheric final warming (SFW) consists in the irreversible break-up of the winter polar vortex, which marks the springtime transition between the winter (cyclonic) and summer (anticyclonic) dynamical regimes in the extratropical stratosphere [*Black and McDaniel*, 2007]. SFWs occur in both hemispheres and their timing and dynamical evolution is ruled by a combination of radiative and planetary wave forcing effects. In the Northern Hemisphere, the enhanced planetary wave activity (due to increased orography and land-sea contrasts) leads to a large SFW inter-annual variability of its timing and vertical structure that in turn can have remarkable consequences in the stratosphere and the troposphere.

In the case of the SFW timing, SFWs onset dates oscillate in a range of about two months and are sensitive to the stratospheric background state apart from the upward-propagating wave activity [*Waugh et al*., 1999; *Salby and Callaghan*, 2007]. The timing of SFWs can have sizeable consequences on the rate of polar ozone depletion and the stratospheric chemical composition in spring and summer [e.g. *Manney et al.*, 2011]. For instance, anomalously early SFWs (i.e. early vortex break-up) can lead to a rapid cessation of ozone loss as it was the case in winter 2004/2005 [*Manney et al*., 2006b; *Manney and Lawrence*, 2016]. *Waugh and Rong* [2002] also showed strong differences in the polar vortex mixing processes with mid-latitude air in association with the SFW timing. More recently, *Thiéblemont et al*. [2011, 2013] revealed that early SFWs are more likely to feature "Frozen-In" anticyclones occurrences in spring and summer [*Manney et al*., 2006a], which lead to anomalously high nitrous oxide and methane concentrations in the polar stratosphere. However, not only does the variability of SFW timing alter the stratospheric composition and circulation, but it also affects tropospheric circulation. *Ayarzagüena and Serrano* [2009] found significant changes in the tropospheric circulation in April, particularly over the Euro-Atlantic sector, when separating between early and late SFWs from ERA-40 reanalysis.

Hardiman et al. [2011] characterized the variability of SFWs by their vertical temporal development rather than their timing: they found that in some years, SFWs occur first in the mid-stratosphere (10 hPa or ~30 km, hereafter referred to as 10-hPa first), and in others SFWs occur first in the upper stratosphere (1 hPa or ~50 km, hereafter referred to as 1-hPa first). They showed that years in which 10-hPa first SFWs occur are associated with a more negative NAO-like pattern in April mean sea level pressure than years in which 1-hPa first SFWs occur. All these results hence demonstrate that the knowledge of the SFW characteristics provides additional predictability skills of springtime tropospheric climate. In this regard, it is important to identify factors that influence the variability of SFWs and to understand the associated mechanisms.

Previous findings based on reanalyses suggested that the variability of SFWs is highly dependent on the stratospheric dynamical conditions in the previous winter. For instance, *Waugh et al.* [1999] found a very strong correlation between the activity of planetary waves entering the stratosphere two months before the SFW (diagnosed as the eddy heat flux at 100 hPa and averaged over the latitude range 45°N-

75°N) and the polar vortex break-up date. *Wei et al*. [2007] related the evolution of the strength of the polar vortex and wave activity during the previous winter to the SFW timing. *Hu et al*. [2014] demonstrated that early spring SFWs (~March) are more likely to be preceded by winters unperturbed by Sudden Stratospheric Warming (SSW) events, while late spring SFWs are mostly preceded by SSW events in mid-winter. *Hardiman et al*. [2011] also found that the vertical profile of the SFW is influenced by the strength of the polar vortex before: a weaker polar vortex tends to favor 10-hPa first SFWs. These various results hence suggest that to better understand the variability of SFWs, it is important to understand the drivers of the stratospheric polar vortex dynamical variability in winter.

Numerous reanalysis and climate model studies have examined the sensitivity of the strength of the boreal stratospheric polar vortex to external and/or remote variability factors in winter such as the Quasi-Biennial Oscillation (QBO), solar irradiance fluctuations, or oceanic variability. *Holton and Tan* [1980] suggested a relationship between the strength of the polar vortex and the phase of the QBO (the "Holton–Tan (HT) relationship"). Specifically, they found that the vortex is weaker on average in the easterly phase of the QBO than in the westerly phase. This relationship has afterwards been supported by modeling studies using atmospheric models with various complexity [e.g. *Calvo et al*., 2007; *Hansen et al*., 2013]. The influence of the QBO on the wintertime polar vortex strength has further been proposed to be modulated by the 11-year solar cycle [*Camp and Tung*, 2007; *Matthes et al*., 2013]. It is also well established that the polar vortex is modulated by the El-Niño Southern Oscillation (ENSO) [see e.g. *Garfinkel and Hartmann*, 2008; *Calvo et al*., 2017 and references therein]. Relationships between sea surface temperature and the winter Arctic stratosphere variability have also been found in other sectors such as the North Pacific [*Hurwitz et al*., 2012] and the Atlantic [*Omrani et al*., 2014]. However, a link between these external or remote factors and the SFW variability has not been established yet.

The stratospheric polar vortex is also expected to change in the future as a result of long-term anthropogenic changes in atmospheric composition, i.e. increasing greenhouse gas (GHG) concentrations and stratospheric ozone layer recovery. For instance, several studies have examined possible trends in the future occurrence of mid-winter stratospheric warmings [e.g. *Bell et al*., 2010; *SPARC CCMVal*, 2010; *Mitchell et al*., 2012; *Hansen et al*., 2014; *Kim et al*., 2017], but no consensus has been reached yet. By applying different metrics to 12 climate models, *Ayarzagüena et al*. [2018] recently came to the conclusion that the occurrence frequency of mid-winter major warmings is not projected to change under anthropogenic climate change. Nevertheless, the effects of projected climate change on SFWs have not been addressed.

Drivers of polar vortex variability and trends, and their associated mechanisms, are, by far, more documented in winter than in spring. The aim of the present study is to improve the understanding of the dynamical variability of SFWs by assessing how the QBO, variable SSTs and anthropogenic emissions modulate their dynamical characteristics; i.e. vertical profile and timing. Note also that the

Commented [u1]: You completely ignore in this section the impact of solar variability on the polar vortex. Why? Its modulation of the HT mechanism has been shown in many studies. It is fine if you don't address solar variability in your SFW analysis but as for mid-winter warmings you should mention it in the introduction. For literature you might check http://www.geo.fu-berlin.de/met/ag/strat/publikationen/index.html

Commented [rt2R1]: I ignored it for conciseness (since we don't investigate the solar signal in SFWs). I now mention it.

Commented [u3]: References?

Commented [rt4R3]: I added some

previous studies which examined the dynamical features of SFWs were essentially based on reanalysis datasets, not on climate model simulations and so, the length of observations is relatively short to derive robust conclusions. Here, we use for the first time multi-decadal integrations (145 years) of a fully coupled chemistry-climate model (WACCM) to investigate SFWs. Such long experiments allow a large statistical sampling. Four sensitivity experiments are analyzed to assess the impact of the external factors.

The paper is organized as follows. Section 2 describes the model, the sensitivity experiments and the definition of the different classifications of SFWs on which the composite analysis is based. Section 3 examines the stratospheric dynamics of SFWs and the associated surface climate response simulated by the model. In section 4, we investigate the relationship between the polar vortex strength in winter and the dynamical evolution of SFWs. Section 5 assesses the influence of the external factors (i.e. QBO, transient SSTs and anthropogenic forcing) on the distribution of SFWs (according to their class) and their timing. A summary of the study is provided in section 6.

Commented [u5]: Has already been said before. I think it fits very well here, so maybe delete the earlier sentence.

Commented [rt6R5]: I agree. I removed the earlier part.

2. Data and methods

2.1 CESM1(WACCM)

The numerical simulations are performed with the Community Earth System Model (CESM), version 1.0.2, developed at the National Center for Atmospheric Research (NCAR). CESM is a fully coupled model which includes an interactive ocean (POP), land (CLM), sea ice (CICE), and an atmospheric component with interactive chemistry (WACCM3.5) [*Marsh et al.*, 2013]. The POP ocean module has a tripolar horizontal grid of 1°×1° and 60 depth levels. WACCM3.5 [*Gent et al.*, 2011] uses a vertical hybrid σ-P coordinate, has 66 levels and a lid-height at ~140 km (~5.1×10^{-6} hPa). The model is integrated with a horizontal resolution of 2.5° in longitude and 1.9° in latitude. Interactive chemistry is calculated with the 3D chemistry module based on version 3 of the Model for Ozone And Related chemical Tracers (MOZART) [*Kinnison et al.*, 2007]. WACCM3.5 is forced by daily spectrally resolved solar irradiance from the NRLSSI1 dataset [*Lean et al.*, 2005].

Commented [u7]: The levels are horizontal.☺

Commented [rt8R7]: Yes, right, it's a common mistake I presume ☺ !

In our model version, the vertical resolution of WACCM is not high enough to internally generate a QBO. Therefore, the modeled tropical zonal winds are relaxed to observations between 22°S and °N using a Gaussian weighting function with a half width of 10° which decays latitudinally from the equator (see *Matthes et al.* [2010] for details). The relaxation extends in the vertical from 86 to 4 hPa with a time constant of 10 days. The equatorial QBO forcing time series is determined from the climatology of 1953–2004 reconstructed from combined radiosonde [*Naujokat*, 1986] and rocket sonde measurements [*Gray et al.*, 2001]. More information on the QBO climatology used for the nudging procedure can be found at http://www.pa.op.dlr.de/CCMVal/Forcings/qbo_data_ccmval/u_profile_195301-200412.html. The filtered spectral decomposition of the climatology gives a set of Fourier coefficients that can be expanded for any day and year in the past and the future.

2.2 Model experiments

To examine the influence of external variability sources on Northern Hemisphere SFWs, four CESM1(WACCM) simulations, spanning 145 years, were performed by systematically switching on and off particular variability factors as summarized in Table 1. All experiments start in January 1955 and run until December 2099. The four model experiments are forced by NRLSSI1 (daily solar spectral irradiance dataset [*Lean et al*., 2005]) from 1955 to 2009. From 2010 to 2099, the solar forcing is prescribed by repeating twice the last four solar cycles provided in NRLSSI1. The three major volcanic eruptions observed, i.e., Agung (1963), El Chichón (1982), and Mount Pinatubo (1991), are included by prescribing the volcanic forcing described in [*SPARC,* 2010].

The Natural experiment simulates the natural variability of climate, i.e. without including anthropogenically induced GHG and ozone concentration changes. This experiment is hence performed by keeping the concentrations of GHGs and Ozone Depleting Substances (ODS) constant at the 1960s level but by including all natural sources of variability such as ENSO or QBO. The RCP85, NoQBO and FixedSST experiments are designed by modifying specific settings of the Natural experiment. In the RCP85 experiment, the observed GHG and ODS concentrations are prescribed until 2005 and the RCP8.5 scenario [*Meinshausen et al*., 2011] is used from 2006 onward. In the NoQBO experiment, the QBO nudging procedure is switched off, leading to weak easterlies throughout the depth of the tropical stratosphere. Finally, in the FixedSST experiment, the ocean interactive coupling is switched off and the SST is instead prescribed based on the seasonal climatology derived from the Natural experiment. Hence, comparing the RCP85, NoQBO and FixedSST experiments with the Natural experiment allows quantifying the effect of anthropogenic forcing, QBO and ocean variability, respectively, on stratospheric final warmings in the Northern Hemisphere.

Name	Period	GHGs/ODSs	QBO	SST/sea ice
Natural	1955-2099	Fixed at 1960s level	Nudged	Interactive
RCP85	1955-2099	**RCP8.5 scenario**	Nudged	Interactive
NoQBO	1955-2099	Fixed at 1960s level	**No**	Interactive
FixedSST	1955-2099	Fixed at 1960s level	Nudged	**Climatological**

Table 1. Summary of CESM(WACCM) Experiments

The analyses of CESM(WACCM) simulations are compared with ERA-Interim products [*Dee et al*., 2011], which provide meteorological reanalyses from 1979 to present and cover the full troposphere/stratosphere region. CESM(WACCM) results are also compared with results of a multi-decadal simulation performed with the EMAC (ECHAM/MESSy Atmospheric Chemistry) chemistry-climate model [*Jöckel et al*., 2006] (140 years) and run under constant 1960s levels of GHGs and ODSs, i.e. comparable to the Natural CESM(WACCM) simulation. In this configuration, EMAC is fully

Commented [u9]: Which ODS scenario do you use for the future?

Commented [rt10R9]: In Meinshausen et al. [2011], The RCP8.5 is provided with a ODSs scenario too.

Commented [u11]: It needs to be specified which EMAC-O simulation was used and to which CESM simulation it can be compared. I think there is no EMAC run with exactly the same setup. Which run did you use?

Commented [BA12R11]: It is the control simulation for 1960 year. The setup is very very similar to the Natural CESM simulation.

Commented [rt13R11]: Thanks Blanca

coupled with the MPI-OM ocean module [*Jungclaus et al*., 2006] (hereafter denoted EMAC-O). The EMAC-O results are shown in the supplementary material.

2.3 Classification of SFWs and composite analysis

The SFW onset date is defined, at each pressure level between 50 and 1 hPa, as the time when the zonal mean zonal wind at 60°N becomes easterly without returning to westerlies until the subsequent autumn [*Hardiman et al,* 2011]. As explained in *Hardiman et al.* [2011], this definition can be applied either on daily or monthly data. Although the use of daily data seems more accurate, in many years the zonal mean zonal wind value at 60°N near the time of the SFW can durably fluctuate around zero before stabilizing to summer easterlies. In that case additional work is required to identify the SFW date. Given the large amount of data to be handled and the good performance of results when dealing with monthly data, we used monthly data that are linearly interpolated to the day where the zonal mean zonal wind crosses the zero line at each level. Once the vertical profile of the SFW date is defined, we classify the type of SFW by comparing the dates at 10 hPa and 1 hPa. If the SFW occurs first at 10 hPa or 1 hPa, then it is labeled as "10-hPa first" or "1-hPa first", respectively. Note that if less than 5 days separate the SFW dates at 10 and 1 hPa, the SFW is classified as "neutral". This classification of SFWs allows considering the full vertical evolution of the springtime transition in the stratosphere [*Hardiman et al*., 2011].

Figure 1 shows the vertical profile of the SFW dates for the (a) 1-hPa first, (b) 10-hPa first and (c) neutral cases. The four CESM(WACCM) experiments are considered together. For 1-hPa first SFWs, the polar vortex initially breaks near the stratopause (i.e. at 1 hPa). In CESM(WACCM), the average timing of the SFW onset at 1 hPa is found at day 52, corresponding to April 22 (Figure 1a). This appears consistent with the average SFW timing found in ERA-I (day 50). On average, the vortex break-up date propagates downward progressively from 1 to 30 hPa in ~20 days in both model and reanalysis. For the 10-hPa first SFWs (Figure 1b), the average timing of SFW onset at 10 hPa in CESM(WACCM) is found at day 49 (i.e. April 19) and shows a comparatively slower downward propagation (i.e. 16 days from 10 to 30 hPa). The average onset of 10-hPa first SFWs is found to occur significantly earlier in ERA-I, at day 40.

In CESM(WACCM) simulations, 1hPa-first SFWs occur (51.4% or 298 cases in total) more frequently than 10-hPa first SFWs (36% or 209 cases in total). A similar distribution is found in the EMAC-O simulation with 56% of 1hPa-first and 32% of 10hPa-first SFWs. This contrasts with ERA-I results that revealed statistically significantly more frequent 10-hPa first SFWs (~55%). Finally, in simulations of both models (CESM(WACCM) and EMAC-O), around 12% of SFWs were classified as neutral SFWs and are not considered thereafter.

Commented [u14]: It would be interesting to add a sentence for the 10 hPa-first SFWs about the delay in vortex breakup date above 10 hPa.
Are there really two separate vortices when the vortex is broken up at 10 hPa but not yet below and above?

Commented [rt15R14]: That's a very good question, but also very complex to answer because, in contrast with 1-hPa first SFWs, which all look quite similar, 10-hPa first can be of various kind. Either the vortex progressively declines simultaneously at 10 and 1 hPa, but more quickly at 10 hPa, which leads to a 10-hPa first SFW. It happens also that the vortex is weakened initially at 1-hPa and 10-hPa, leading to definite easterlies reversal at 10-hPa but not at 1-hPa, where it takes longer (due sometimes to partial recovery). The variability of the polar vortex is far from being simply binary, but is rather a continuum. This appears clearly when we look at PV maps evolution. The criteria we use allows defining an "average" behavior, but by doing so, we also somehow restrict the actual complexity of the vortex breaking. I'd prefer avoiding this complex discussion to avoid confusing the reader. Note that in a previous version, I added a very long paragraph on SFW definition criteria (basically reviewing various aspects). Blanca and I however decided to remove it to sharpen the text (I think it was a good solution).

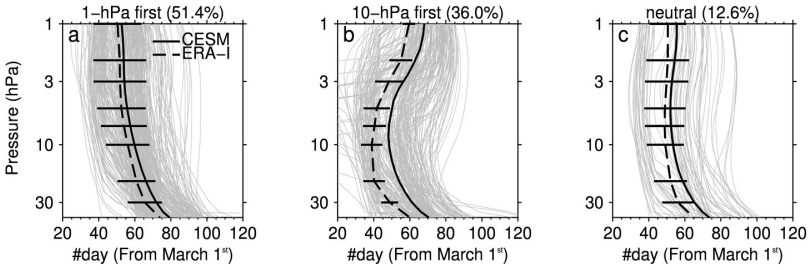

Figure 1. Vertical profile of the vortex break-up date (see text for detail) for all final warmings simulated by the model (480 in total, thin gray profiles) classified as (a) 1hPa-first, (b) 10hPa-first and (c) neutral. The solid (dashed) black line indicates the average of all profiles for the model (ERA-I reanalysis). Error bars indicate the 2σ standard error from the mean for ERA-I.

In this study, we perform a composite analysis to examine the atmospheric circulation perturbations and responses associated with the 1-hPa and 10-hPa first SFWs. The central dates of the SFWs are defined as the vortex break-up date (see Figure 1) at the 1 hPa and 10 hPa levels for the 1-hPa and 10-hPa first cases, respectively. The composites for a given SFW type are constructed by averaging together all the fields and/or fields anomalies derived for each SFW of the same type. Here, monthly/daily *anomaly* refers to *deviation from the corresponding calendar monthly/daily climatology*. The statistical significance of the composites is estimated using a bootstrapping technique; i.e. random sampling with replacement [*Mudelsee*, 2014]. The procedure is to select a random subset from the original time-dependent dataset with the number of samples equal to the original composite subset. We reiterate the procedure 1,000 times to build a probability density function (PDF), which is then used to determine the likelihood of the derived signals to arise by chance. For two dimensional fields, the procedure is done at each grid point independently. Two-tailed tests are employed.

Commented [u16]: I don't understand what the climatology is from which you derive anomalies for the composite. The composite does not have an absolute date. Which date do you use for the climatology then to determine the anomaly? Do you have to construct the climatology somehow and how?
Or is this just the winter mean?

Commented [BA17R16]: Modified! It is the calendar day or month depending on the case. This allows us to obtain deseasonalized anomalies.

Commented [rt18R16]: Yes, thanks Blanca for clarifying.

To explore the influence of the wintertime dynamical evolution on the following springtime SFW characteristics, the frequency and timing of SSWs are also analyzed. SSWs are identified by the simultaneous reversals of the zonal mean zonal wind at 10hPa and 60°N and the zonal mean temperature difference between 60°N and the pole [*Labitzke,*1981]. Note that these particular criteria define *Major* SSWs, that we thereafter refer to as SSWs for sake of simplicity. The winter season is defined from 1 November to 15 days before the SFW central date in order to avoid any overlap between the SFW and SSWs.

3. Dynamical evolution during SFW

We first examine the stratospheric dynamics and the surface climate response associated with the 10-hPa and 1-hPa first SFWs in the four CESM(WACCM) model simulations. Note that in this and the next section, the composite analysis combines all the experiments together as the atmospheric

dynamical changes associated with the SFW lifecycle were found to be nearly independent of the experimental setting.

3.1 Stratospheric dynamics

Figure 2 shows the anomalous stratospheric dynamical state for the 10 days before the onset of the 10-hPa and 1-hPa first SFWs. Before the onset of 10-hPa first SFW (Figure 2a), the zonal mean zonal wind anomalies are negative throughout the depth of the polar stratosphere (northward of 60°N) with a minimum of -10 $m \cdot s^{-1}$ centered at 75°N and 5 hPa (~40 km). This clearly indicates an anomalously weak polar vortex before the SFW. Conversely, the 1-hPa first cases display positive zonal mean zonal wind anomalies in the polar stratosphere up to 3hPa before the SFW, denoting an anomalously strong polar vortex, and negative values higher up that represent the start of the polar vortex break-up (Figure 2b). In the tropical stratosphere, for the 10-hPa first case, the zonal mean zonal wind anomalies show anomalous westerlies (6 $m \cdot s^{-1}$), easterlies (-2 $m \cdot s^{-1}$), centered at 20 hPa, 50 hPa, respectively. In the 1-hPa first case, the opposite (but with a reduced magnitude) is found with anomalous easterlies at 20 hPa (-4 $m \cdot s^{-1}$) and westerlies at 50 hPa (1 $m \cdot s^{-1}$). This hence would suggest a possible influence of the phase of the QBO on the SFW type in CESM(WACCM).

Figure 2c and d show the anomalies of planetary wave propagation and wave mean-flow interactions diagnosed by the Eliassen-Palm flux (EPF, vectors) and its divergence (contour). We recall that an anomalous convergence of EPF (or negative anomaly) leads to an enhanced wave drag and thus a relative westward acceleration of the zonal flow. Before the 10-hPa first SFW (Figure 2c), an anomalous increase in upward wave propagation is seen at high latitudes in the stratosphere. This increase in wave activity triggers an anomalous EPF convergence (i.e. enhanced wave breaking) which maximizes (0.8 $m \cdot s^{-1} \cdot d^{-1}$) near 75°N and between 30 and 5 hPa. The wave induced westward acceleration at these altitudes hence participates in the westerly-to-easterly reversal of the wind that defines 10-hPa first SFWs. For the 1-hPa first SFWs, the wave activity anomaly entering the stratosphere is stronger and concentrates in a narrower latitude band which is centered at 65°N (Figure 2d). In comparison with the 10-hPa first cases, the EPF convergence anomaly for the 1-hPa first cases is also substantially larger (more than 2 $m \cdot s^{-1} \cdot day^{-1}$) and localized at higher levels (above 3 hPa), in the stratopause region. This is consistent with the negative zonal mean zonal wind anomalies found in the upper polar stratosphere (Figure 2b).

Commented [u19]: Do you have an explanation why in the 1 hPa-first SFWs a much stronger EPF in the upper stratosphere causes a weaker westward acceleration than the 10 hPa-first SFWs?

Commented [rt20R19]: Panels a and b do not give indication of the acceleration, but rather of the anomalous state of the zonal mean zonal wind associated with each SFW type. I checked the acceleration from -15 to 15 days around the SFW central date and I found that the westward acceleration is indeed stronger for 1-hPa first cases, which is consistent with the EP-flux convergence values.

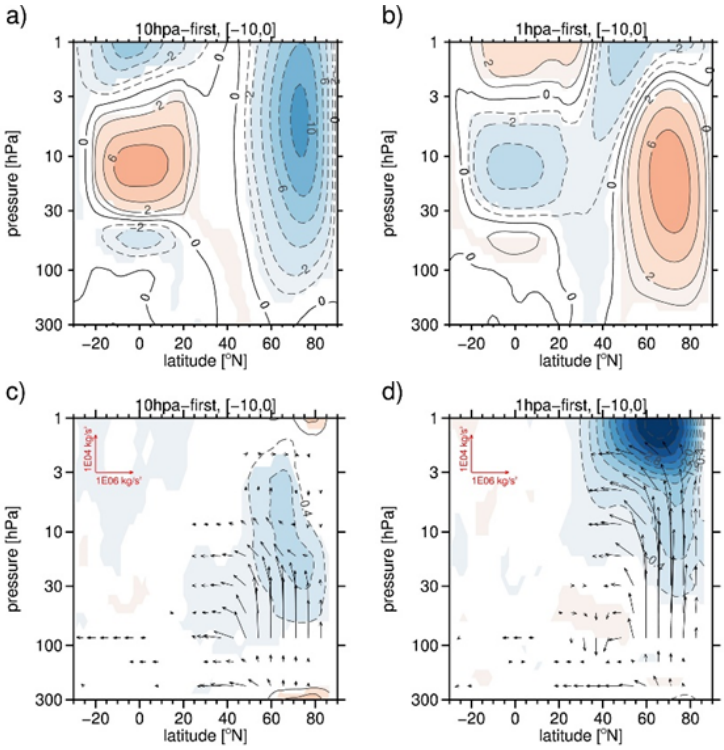

Figure 2. Zonal mean zonal wind anomaly (contour, drawn every 2 ms^{-1}) associated with the (a) 10-hPa first and (b) 1-hPa first cases averaged from -10 to 0 days relative to the SFW central date. (c,d) as for (a,b) but for the Eliassen-Palm flux (vectors, scales and units are shown on the upper left of each panel) and its divergence (contours, drawn every 0.4 $ms^{-1}d^{-1}$) anomalies. Shading indicates regions where anomalies are statistically different from zero at the 95% confidence level.

Commented [BA21]: I think the scale arrow is missing. I would also include the units.

Commented [rt22R21]: done

Commented [BA23]: Include contour interval with units.

Commented [rt24R23]: done

The stratospheric dynamical characteristics prior to SFWs in our simulations are found to be consistent with *Hardiman et al*. [2011], which were based on ERA-I reanalysis dataset. Their analysis further revealed that SFWs were followed by significant perturbations of the troposphere circulation. The following section focuses on the surface signals associated with the different SFW types and their effect on regional climate in our CESM(WACCM) simulations.

3.2 Surface Signals

The evolution of the 10-day average sea level pressure (SLP) anomalies around the onset of the SFWs is shown in Figure 3. No significant SLP signal is found during the period preceding 10-hPa first SFWs (Figure 3a). Within the 10 days following 10-hPa first SFWs (Figure 3b), a high pressure anomaly

(greater than 1 hPa) starts to develop over the polar cap, accompanied with low pressure anomalies over Europe and east Asia. The high pressure anomaly then further enlarges and persists throughout the following month (Figure 3c-e) while the low pressure anomalies vanish earlier (days 20-30, Figure 3d). The evolution of the SLP anomalies associated with 1-hPa first SFWs markedly differs. Before the onset of 1-hPa first SFWs (Figure 3f), the SLP signal shows clear negative anomalies extending over the polar cap and Greenland and positive anomalies at mid-latitudes that encompass the East Atlantic-European sector, Northern Asia and the North Pacific. This pattern, which strongly resembles the positive phase of the Arctic Oscillation, then progressively vanishes within the month following the 1-hPa first SFW (Figure 3g-j). Note that for both types of SFWs, the sea level pressure anomaly evolves similarly (trending toward a more negative North Atlantic/Arctic Oscillation) despite different tropospheric initial situations as shown by the temporal evolution of Figure 3a-to-e and Figures 3f-to-j. Hence, this suggests that there are no different stratosphere-troposphere processes at work between the two types of SFWs, but rather an offset in the surface signals.

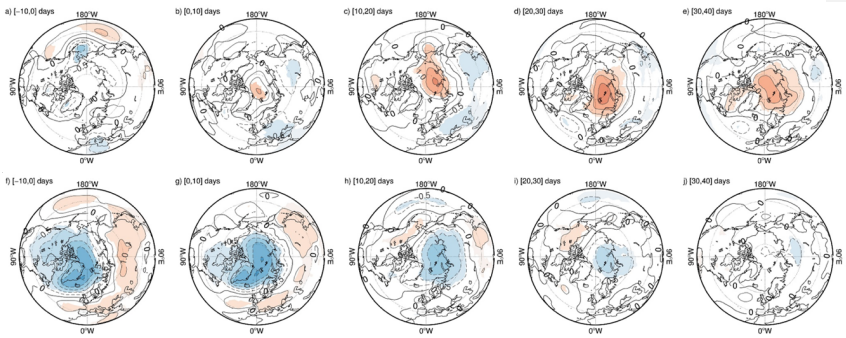

Figure 3. Sea level pressure anomaly associated with the 10-hPa first cases (top) and 1-hPa first cases (bottom) averaged in the ranges [-10,0], [0,10], [10,20], [20,30] and [30,40] days relative to the SFW central date. All experiments are considered together. Contours are drawn every 0.5 hPa. Shading indicates regions where anomalies are statistically different from 0 at the 95% confidence level.

A similar SLP analysis has also been conducted with the EMAC-O simulation and ERA-I data (Figs. S1, S2). EMAC-O results show a temporal and spatial response similar to that of CESM(WACCM). In ERA-I, although the anomalies appeared consistent with those of CESM(WACCM) for the 1-hPa first cases, the statistical significance is substantially reduced. For the 10-hPa first cases, no clear signal could be identified. This may suggest that, at this 10-day timescale, a relatively large sample is required for the signal to be identified and overcome the inter-annual variability. We examined the effect of the sampling size on the strength of the signal and its significance in our CESM(WACCM) experiments. Figure 4 shows how the sampling size (number of years used to perform the composite analysis) affects the signal in SLP anomalies averaged northward of 85°N and from 0 to 10 days relative to the SFW

Commented [u25]: Siberia?

Commented [rt26R25]: Thanks for noticing, it's rather East than West Asia, but not really Siberia to me.

Commented [u27]: Do you have an explanation for the differences in both SFWs? Is it just the different SLP starting position that leads to different wave forcing of the stratosphere and hence different ST feedbacks?
As in both cases, a positive trend develops in the Arctic, could that also be a radiative response to the seasonal cycle?

Commented [rt28R27]: I examined the daily evolution of the slp anomaly over the polar cap and the evolution seems not to be exactly similar in both cases: i.e. the positive trend in the case of 10-hPa first is abrupt just after the SFW, and then evolves more gently, while in the case of 1-hPa first, the positive trend evolves monotonically. But, the significance of these different behaviors remain to establish, and seems to be of second order suggesting that no strong different mechanism is at work: just a similar evolution but starting from different initial situation in the troposphere as you mention. Thanks for your input. I tried to add some explanation at the end of the paragraph. Hope it's clear

Commented [u29]: To be honest: after having looked at the nice figure 3 for a while, it is a nightmare to look at Figs. S1 and S2.
They are so different in style that it needs extra switching between the docs for the comparison. It is also really difficult to detect the message (signals) in the S figures. I really recommend to use the same software for both figures or redraw the S figures at least with the same colours (without green continents!), or if not possible, remove the S figures and mention the EMAC-O and ERA-I results in the text only.

Commented [rt30R29]: You're right, supplementary figures have been changed accordingly.

Commented [u31]: Only in a), b)?

Commented [rt32R31]: No, all, you're right.

onset (corresponding to panels b and g of Figure 3). For each sample size *n* (spanning from 10 to 570 years by increment of 10 years), we randomly select *n* years from which we calculate the 1hPa and 10hPa-first composite anomalies. This procedure is repeated 1,000 times for each *n*, allowing to construct distributions of the average composite values. The results show that a sample of more than 350 years is needed to have more than 97.5% chances to obtain positive SLP averaged anomalies 10 days after the 10 hPa-first SFWs (red) in our model. For the 1 hPa-first SFWs (blue), more than 120 years are needed to have more than 97.5% chances to obtain negative SLP averaged anomalies. Even if the model and reanalysis are not directly comparable since the SLP variability and the rate of 10 hPa and 1 hPa-first SFW years are different, these results suggest that large samples are needed to obtain a robust SLP signal associated with the type of SFW and may partly explain why the signals are not well identified in the ERA-I dataset.

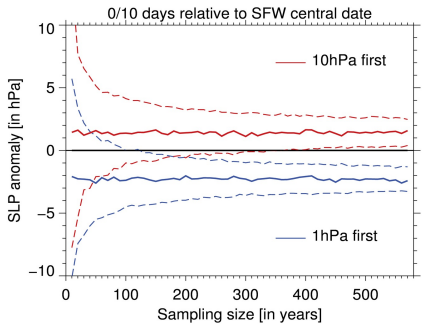

Figure 4. SLP anomalies averaged northward of 85°N and from 0 to 10 days after the SFW onset as a function of the number of years sampled. Each is based on 1000 random realizations. The solid line shows the average and the dashed line the 2.5 and 97.5% percentiles.

Although the analysis of the signals relative to the central date of SFWs provides relevant insights regarding the dynamical evolution of the near-surface circulation associated with SFWs, it does not quantify the sub-seasonal surface climate impact of SFWs that are important for seasonal forecast. Since both types of SFWs are more likely to occur in April (Figure 1), we now examine the springtime SLP and surface temperature anomalies calculated as the difference between years featuring 1-hPa first SFW and years featuring 10-hPa first SFW. Results for April and May are shown on Figure 5.

Commented [u33]: ? surface climate?

Commented [rt34R33]: Corrected (thanks Blanca)

Commented [u35]: Is this the monthly SLP average of all Aprils in which a 1-hPa or 10 hPa-SFW occurred?

Commented [rt36R35]: I tried to clarify.

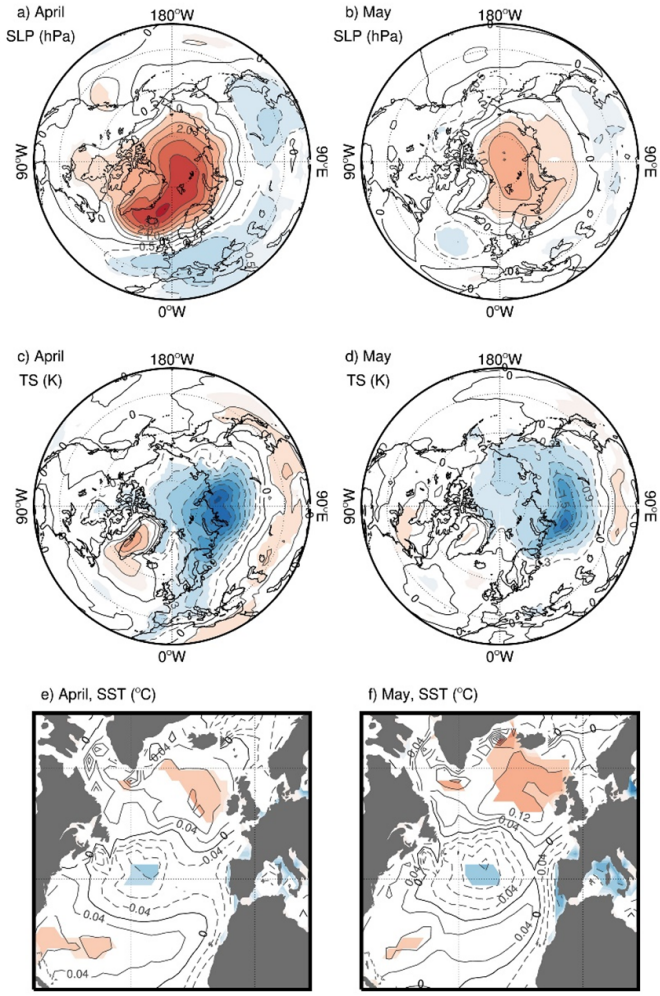

Figure 5. Difference between 10-hPa and 1-hPa first cases of the (a,b) sea level pressure, (c,d) air surface temperature and (e,f) sea surface temperature in (a,c,e) April and (b,d,f) May. All experiments are considered together, except for (e,f) where FixedSST is discarded. Contours are drawn every (a,b) 0.5 hPa, (c,d) 0.3 K and (e,f) 0.04 K. Shading indicates regions where differences are statistically significant at the 95% confidence level.

In April (Figure 5a), the SLP mean difference between 10-hPa and 1-hPa first SFWs reveals a pattern similar to the negative phase of the North Atlantic Oscillation/Arctic Oscillation, with a maximum

Commented [u37]: Again, the EMAC-O plots are in my view not acceptable for a publication. They even show a different latitude section.

Commented [rt38R37]: Indeed, this is now corrected.

positive pressure anomaly greater than 3 hPa over the polar cap/Greenland and minimum pressure anomalies of -1 hPa at midlatitudes. These atmospheric circulation perturbations lead to substantial surface temperature changes at regional scale with cold anomalies lower than -1°C over Northern Eurasia, and moderate (but statistically significant) warm anomalies over Greenland and Southern Eurasia (Figure 5c). In May, similar but weaker responses are found in SLP (Figure 5b) and surface temperature (Figure 5d). CESM(WACCM) results are consistent with EMAC-O (Figure S3) and ERA-I [*Hardiman et al*., 2011], which reveal similar NAO-like signals associated with the SFW type.

Atmospheric circulation changes associated with the NAO affect the underlying Atlantic Ocean by modulating surface air temperature, atmosphere-ocean heat fluxes, as well as mid-latitude wind stress [*Visbeck et al*., 2003]. This induces sea surface temperature anomalies that we examined on Figure 5e,f. In April (Figure 5e), the SST signal is characterized by warm anomalies in the North Atlantic (50-60°N) and subtropical North Atlantic (~30°N), and cold anomalies at mid-latitudes (~40°N). This tripolar SST pattern agrees well with the typical oceanic response to negative NAO-like atmospheric anomalies [*Czaja and Frankignoul*, 2002]. In May (Figure 5f), we obtained a similar SST signal which is further amplified at mid and high latitudes. This is the first time that a SST signal is related to stratospheric final warming onsets. Nevertheless, the statistical significance of this SST tripole is relatively weak despite the large sample (435 years since the FixedSST experiment is not included). This may partly explain the absence of a signal in the observations (not shown).

In this section, we have shown that the two different types of SFWs are linked to significant regional climate perturbations in the Northern Hemisphere which may contribute to a better understanding of inter-annual climate variability in spring. Given the markedly different stratospheric dynamical conditions preceding the two types of SFWs (e.g. Figure 2), we further examine in the next sections whether the stratospheric dynamical evolution throughout the previous winter and the influence of external stratospheric variability factors can provide insights on the spring SFW transition. In other words, can we identify a stratospheric preconditioning that could help predicting the type of SFW?

4. Influence of preceding winter on SFWs

To investigate the stratospheric dynamical preconditioning, we first analyze the zonal flow anomalies in late winter preceding 1-hPa and 10-hPa first SFWs. Figure 6 shows the zonal mean zonal wind anomalies in March associated with 1-hPa and 10-hPa first SFWs in CESM(WACCM) and ERA-Interim. Anomalously strong and statistically significant westerlies, with zonal mean zonal wind speed greater than 5 $m \cdot s^{-1}$ from 30 hPa to 1 hPa, are found in the polar stratosphere in March for years featuring 1-hPa first SFWs (Figure 6a,b). This finding is robust across CESM(WACCM) and ERA-interim (and EMAC-O, see Figure S4), hence supporting that the polar vortex is anomalously strong during the late-winter period which precedes 1-hPa first SFWs. Inversely, the polar vortex preceding 10-hPa first SFWs is anomalously weak as revealed by the strong and significant easterly anomalies (Figure 6c,d).

In the tropical stratosphere, the zonal mean zonal wind anomalies associated with SFW types markedly differ between model and reanalysis. CESM(WACCM) composites show that, for 1-hPa SFWs (Figure 6a), the tropical stratosphere is dominated by easterlies at 10 hPa and westerlies at 50 hPa, and the opposite for 10-hPa SFWs (Figure 6c). Note that this tropical zonal mean zonal wind anomaly is identically found in the three CESM(WACCM) sensitivity experiments with a nudged QBO (i.e. Natural, RCP85 and FixedSST) when we analyze them separately (not shown). Thus, this indicates that in CESM(WACCM) simulations, the easterly - westerly - phase of the QBO (defined at 50 hPa) favor 10-hPa - 1-hPa - first SFWs. In contrast, in ERA-I, no QBO-like signature is found in relation with SFW types. EMAC-O results neither evidence links between the QBO phase and the type of SFWs (Figure S4). The relationship between the QBO and SFWs, as suspected in light of CESM(WACCM) results, is thus not robust and shows a clear model dependency.

Commented [u39]: But it is interesting that EMAC-O has an anomaly pattern more similar to ERA-I. The QBO signal seems to be pretty dominant in CESM.

Commented [rt40R39]: I won't discuss the similarities between EMAC-O and ERA-I tropical pattern as the statistical significance of the signals is too weak. But It is clear that both show no QBO signal, in contrast with CESM(WACCM), where the QBO signal is clear.

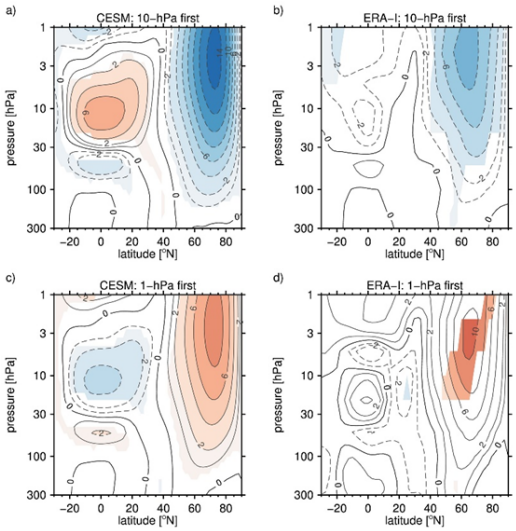

Figure 6. Composite of zonal-mean zonal wind anomalies in March for the (a,b) 1-hPa first and (c,d) 10-hPa first SFW years. (a,c) and (b,d) show CESM(WACCM) and ERA-Interim results, respectively. Shading indicates regions where anomalies are statistically different from the climatology at the 95% confidence level.

Given the relationship between the preceding polar vortex strength in late winter and the type of SFW later on, any factor modulating the polar vortex in winter may thus indirectly affect spring SFWs. Since SSWs are the primary driver of polar vortex strength variability in winter, we now investigate whether there is a relationship between their occurrence in winter and the type of SFWs in spring.

Commented [BA41]: I would put x-axis with the same scale in a, b, d and e. It will allow a better comparison between the model and the reanalysis. I think the peaks of the distribution are not that different in both data sets.

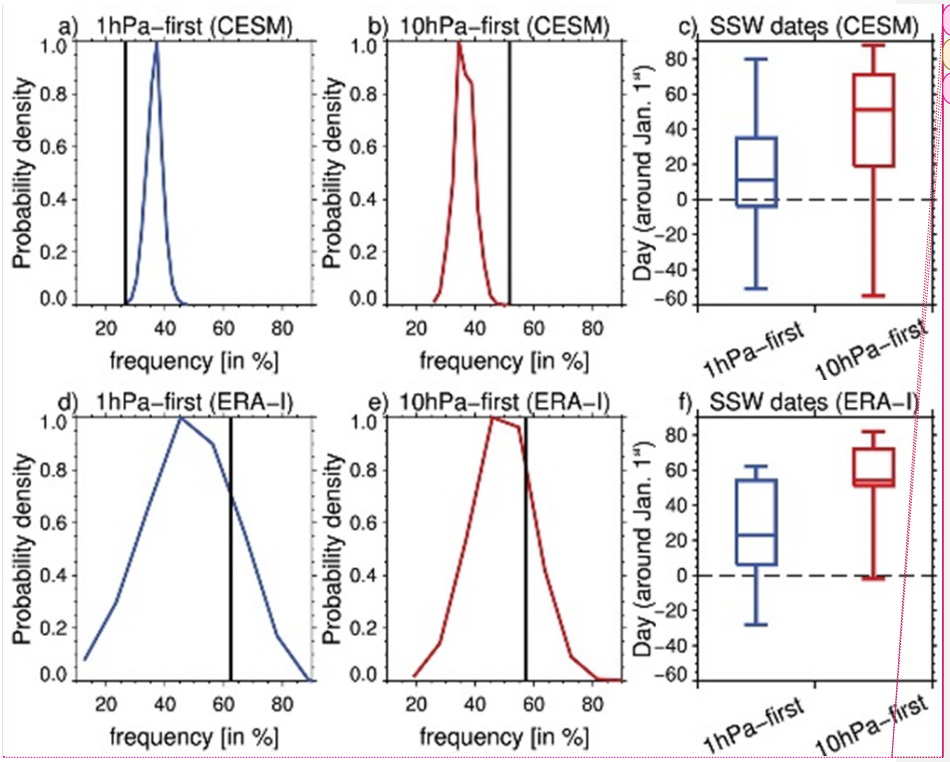

Figure 7. (a,b,d,e) Monte-Carlo test of the likelihood (expressed in %) that at least one SSW occurred during winter using 10,000 synthetic time series generated with random assignments of the SFW type but preserving the same number of years in each group (i.e. (b) 209 for 10-hPa first and (a) 298 for 1-hPa first in CESM(WACCM)) among the total number of years (i.e. 580). The vertical solid line indicates the likelihood when the (a,d) 1-hPa and (b,e) 10-hPa first years are sampled. (c,f) Box diagram of the SSW central date (see text for details) for the 1-hPa and 10-hPa first cases. Panels (a,b,c), and (d,e,f) show CESM(WACCM) and ERA-Interim results, respectively.

Figure 7 examines the link between SSW characteristics (i.e. frequency and timing) and the type of SFW for CESM(WACCM) and ERA-I. As shown by the probability distributions, if years are sampled randomly (i.e. independently of the SFW type), there is a climatological probability of ~37% to have at least 1 SSW per winter in CESM(WACCM) (peak of the distributions in Fig. 7a,b) and ~50% in Era-I (peak of the distribution in Fig. 7d,e). Note that the large difference between CESM(WACCM) and ERA-I is consistent with the anomalously strong polar vortex bias (also referred to as "cold pole bias") in CESM(WACCM), which makes SSWs less frequent [*Marsh et al*., 2013]. If, instead, the sampled years are not randomly distributed but defined according to the nature of the SFW, the chances that at

Commented [rt42R41]: done

Commented [u43]: In the figure: hpa should be hPa

Commented [rt44R43]: done

Commented [u45]: Isn't the climatological likelihood 1 SSW in 2 winters?

Commented [BA46R45]: I find it confusing too.

Commented [rt47R45]: I removed the sentence and tried to make things clearer. Hope it's ok now.

least 1 SSW occurs over the previous winter decrease to 26% in CESM(WACCM) for the 1-hPa first case (vertical line in Fig. 7a), and increase to 52% in CESM(WACCM) for the 10-hPa first case (vertical line in Fig. 7b). These probability frequencies are significantly different from the climatological likelihood at the 95% confidence level. This indicates that, in our CESM simulations, winters with and without SSW are more likely to be followed by 10-hPa and 1-hPa first SFWs, respectively. Such a relationship is also found in EMAC-O results (see Figure S5). Note that winters featuring more than one SSW occurrence further increase the likelihood of a 10-hPa first SFW to occur in spring (not shown).

The timing of the SSWs also impacts the type of SFW. Figure 7c shows the distribution of central dates of SSWs occurring for 1-hPa (blue) and 10-hPa (red) SFWs in CESM(WACCM). Note that if several SSWs occur over one winter, only the central date of the latest one is included in the distribution. This analysis demonstrates that SSWs recorded in winters preceding 1-hPa first SFWs are more likely to occur significantly earlier in the season than for the case of 10-hPa first SFWs. Again, this finding is confirmed in EMAC-O results (see Figure S5). Hence when a SSW occurs in early winter, despite the break-up of the polar vortex, the relatively long time lapse before spring allows the recovery of a strong polar vortex (through radiative processes), which thus favor the occurrence of 1-hPa first SFW. In contrast, if a SSW occurs in late winter, the polar vortex recovery through radiative processes is less efficient since the net radiative heating meridional gradient is less pronounced (see e.g. *Mlynczak et al*. [1999]). As a consequence, the polar vortex is more likely to remain weak until spring, hence favoring the occurrence of 10-hPa first SFW.

We also examined the link between the occurrence of SSWs in winter and the type of SFW using ERA-I, but no relationship is found (Figures 7d,e). Analogously to the SLP analysis presented in section 3, we tested the influence of the sampling size on the significance of the relationship between SSWs in winter and the type of SFW using CESM(WACCM) data. Results are shown on Figure 8. As expected, the spread of the probability distribution that at least 1 SSW occurs before each type of SFW tightens with increasing sample size. The results also show that samples of more than 150 years are required to have more than 97.5% likelihood that the frequency of SSWs before 10 hPa first (red) and 1 hPa first (blue) differs from the climatological frequency (i.e. 37%). The relatively short period covered by ERA-I may thus partly explain the absence of detection of SSW/SFW type relationships. Nonetheless, analysis of ERA-I suggests a relationship between the SSW timing and the SFW type which is consistent with the model results (Figure 7f): SSWs recorded in winter preceding 1-hPa first SFWs are more likely to occur earlier in the season than for the case of 10-hPa first SFWs.

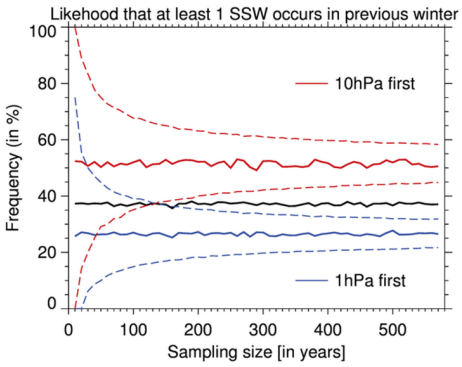

Figure 8. Probability that at least 1 SSW occurs in previous winter for (black) random years sampling, (red) 10-hPa first years sampling and, (blue) 1-hPa first years sampling as a function of the number years considered. Each is based on 1,000 random realizations. The solid line shows the average and the dashed line the 2.5 and 97.5% percentiles.

In this section, model results demonstrated that the dynamical variability of the polar stratosphere during winter has a significant impact on the development of SFW recorded later in spring. The next section focuses on the influence of external sources of variability and forcings on SFW.

Commented [u48]: Why internal? You analysed all simulations including the external sources, right? Maybe 'dynamical'?

Commented [BA49R48]: I agree with Ulrike.

Commented [rt50R48]: I changed internal for dynamical

5. Influence of remote variability sources on SFWs

As developed in the introduction, it is well established that the stratospheric polar vortex can be influenced by external variability sources such as e.g. ENSO [e.g. *Butler et al*., 2014], QBO [e.g. *Watson and Gray*, 2014] or anthropogenic emissions [e.g. *Ayarzagüena* et al., 2018]. Since we demonstrated in the previous section that the type of SFW is significantly connected to the strength of the polar vortex, SFWs variability should also be linked to these external variability sources. In this regard, we now examine the influence of the different experimental settings (i.e. FixedSST, NoQBO and RCP85) on SFWs in our CESM(WACCM) simulations.

5.1 Frequency

Figure 9a shows the distribution of the type of SFW as a function of the experimental setting. The most important changes in SFW distribution are found in the FixedSST and NoQBO simulations. Removing the interannual SST variability leads to a substantial increase/decrease of the 1-hPa/10-hPa first SFWs frequency (+18%/-17%) compared to the Natural experiment. This difference is statistically significant at the 95% level according to the χ^2 test. Conversely, removing the QBO variability triggers a decrease/increase of the 1-hPa/10-hPa first SFWs frequency (-7%/+12%) compared to the Natural experiment (significant at the 90% level). Note that the NoQBO experiment is the only simulation showing more frequent 10-hPa first than 1-hPa first SFWs (+10%). The NoQBO SFW distribution is

significantly different from the FixedSST one at the 99% confidence level. In the RCP85 experiment, the distribution of SFWs shows no significant difference with the natural experiment. We further investigated whether the distribution of SFWs in the RCP85 could change in time but no significant trend was found. Note that an average frequency of ~10% of neutral SFWs is found, independently of the experimental setting.

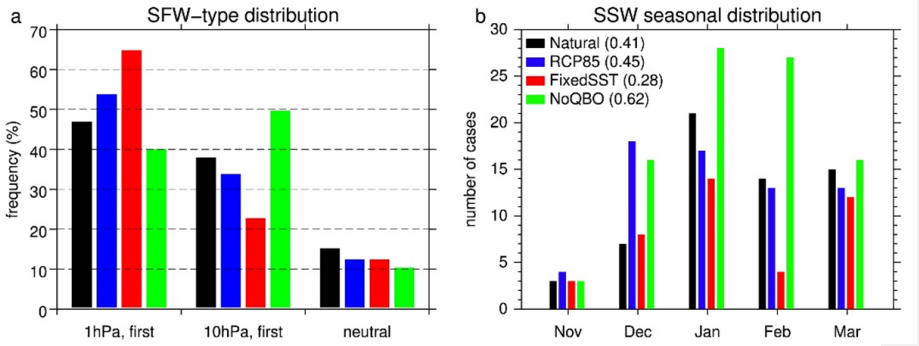

Figure 9. (a) Distribution of the type of final warming and (b) seasonal distribution of SSWs in the (black) Natural, (blue) RCP85, (red) FixedSST and (green) NoQBO experiments.

Commented [u51]: Are you sure that the March SSWs are no SFWs?

Commented [rt52R51]: Yes, I added some criteria to avoid possible overlaps (see section 2.3).

Given the relationship found between the type of SFW and the occurrence of SSWs in the preceding winter (Figure 7), we further investigate the influence of the remote variability sources on SSWs. Figure 9b shows the seasonal distribution of SSWs for the four different experiments. Overall, removing the QBO leads to a substantial increase of SSWs frequency (6.2 SSWs/decade in the NoQBO experiment compared to 4.1 SSWs/decade in the Natural experiment), while removing the inter-annual SST variability leads to decrease of SSWs frequency (2.8 SSWs/decade in the FixedSST experiment). The most pronounced differences in SSW frequency between the experiments are found in December, January and February, (DJF) which correspond to the months when SSWs timing has a prominent impact on the type of SFWs (Figure 7c). The important increase of SSW events in DJF is hence consistent with the enhanced occurrence of 10-hPa first SFWs in the NoQBO experiment. In the FixedSST experiment, the dramatic reduction of SSWs in February is also consistent with the increased occurrence of 1-hPa first SFWs.

The influence of the external variability sources on the seasonal climatological evolution of the extratropical zonal mean zonal wind is further investigated on Figure 10. It shows the differences of the FixedSST (panel a), NoQBO (panel b) and RCP85 (panel c) simulations with the Natural experiment. Constraining the model with climatological SSTs (Figure 10a) leads to a substantial strengthening of the polar vortex which is found particularly pronounced in late winter/early spring with differences greater than 4 m/s from January to April between the Natural and FixedSST experiments. The strong

vortex anomalies in this period are in turn consistent with the significant increase (decrease) of 1-hPa (10-hPa) first SFWs in the FixedSST experiment. Note that the lessened disturbance of the polar vortex in the FixedSST experiment is also consistent with missing variability sources in the troposphere which results in reduced upward wave propagation and decreased wave dissipation/breaking in the stratosphere.

Removing the QBO (i.e. replaced by weak easterlies in the tropical lower stratosphere) is found to have less impact on the polar night jet strength than removing the variable SSTs (Figure 10b). In the NoQBO experiment, the polar night jet appears climatologically weaker than in the Natural experiment namely in mid-winter (i.e. DJF) but the differences are only marginally significant. In spring, no differences are found between both experiments.

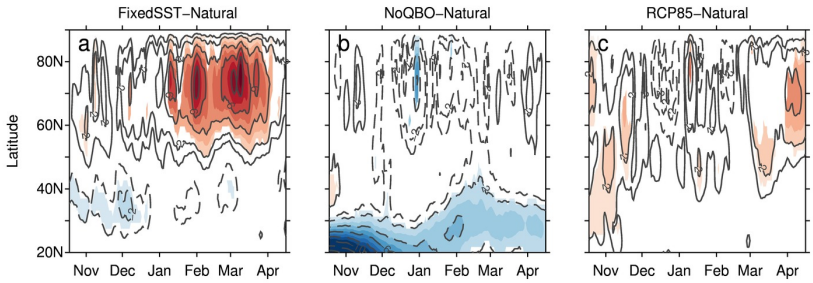

Figure 10. Differences of daily climatology of 10 hPa zonal mean zonal wind from November to April in the Northern Hemisphere between (a) FixedSST, (b) NoQBO, (c) RCP85 and the Natural experiment. Solid (dashed) contours indicate positive (negative) anomalies and are shown with intervals of 1 m s^{-1}. Shading indicates that differences are statistically significant at the 95% confidence level (two-tailed Student's *t*-test).

The polar night jet anomalies associated with the RCP85 scenario show an overall strengthening (Figure 10c), which is statistically significant in early winter (i.e. October/November) and spring (i.e. March/April). These two periods of seasonal transitions in the stratosphere – when the polar vortex forms and disrupts, respectively – are particularly sensitive to radiative effects. Despite the absence of an effect on SFW distribution changes, these anomalies may still affect the timing of SFWs that we examine in the next part.

5.2 Timing

Previously we showed that in CESM(WACCM) the SFW onset occurs on average on April 22 and April 19 for 1-hPa first and 10-hPa first cases, respectively (Figure 1). As shown on Figure 11, the timing of SFWs is however sensitive to natural and anthropogenic external drivers. In the Natural and RCP85 experiments, 10-hPa first SFWs occur on average 7-8 days earlier than 1-hPa first SFWs. This behavior

Commented [u53]: Lubis et al 2016 address the wave reflection in the stratosphere. However, the fact that the polar vortex is stronger with fixed SSTs might simply be an effect of missing variability SOURCES in the troposphere.

Commented [BA54R53]: I agree. I think this is included in the reduced upward wave propagation. Maybe it should be stated more clearly.

Commented [rt55R53]: I modified the sentence accordingly and removed the reference to Lubis et al. [2016].

Commented [u56]: Fig 10c implies that the polar vortex breaks down later in the RCP8.5. We don't see this in EMAC (Fig. 6 in Langematz et al., 2014). While it forms earlier in autumn in the future, it is **not** more persistent in spring due to a future increase in tropospheric dynamical forcing in late winter.

Commented [BA57R56]: Uhmmmm well… we do see a similar strengthening of the climatological zonal mean zonal wind at 10hPa in late winter in EMAC runs (Ayarzagüena et al. 2013). I have seen in Langematz et al. (2014) that the dates of SFWs are computed based on the zonal wind transition at 50hPa that remains below 10m/s. I can also remember that SSWs in RCP8.5 in EMAC tend to happen much later by the end of 21st century. Thus, I guess that one reason for the disagreement between Langematz et al. (2014) and the results here or at least in Ayarzagüena et al. (2013) might be that future SSWs take place later (we see a weakening although not stat. significant in February) and the polar vortex does recover after that at 10hPa but it does not clearly do it at 50hPa (I find the threshold of 10m/s a bit too high for identifying a SFW (it corresponds to approximately half of the climatological value in DJF)).

Commented [rt58R56]: I looked at the zonal wind evolution in the two experiments and the differences between them is more pronounced from 1980 to ~2050 => the vortex is stronger in the RCP85 experiment and this contributes to the anomaly found in Fig. 10c. This is consistent with Figure 12a showing the delayed vortex breakup near the ozone minimum (for 1hPa first).

Although (as mentioned by Blanca), it's not easy to compare with the results of Figure 6 of your 2014 paper since the criteria are quite different, it seems still that in 2000 conditions, the vortex breakup date is delayed too.

is consistent with reanalysis results (see. Figure 1). The premature occurrence of 10-hPa first SFWs compared to 1-hPa first SFWs is also seen in the FixedSST experiment, although the timing difference is substantially reduced and not statistically significant. Finally, in the NoQBO experiment, the averaged timing between both types of SFWs shows no difference. Furthermore, the averaged timing of the 10-hPa first SFWs appears anomalously late in the NoQBO experiment compared to the Natural, RCP85 and FixedSST experiments. This is consistent with the anomalously strong high latitude westerlies found in April in the NoQBO experiment compared to the other experiments when solely 10-hPa first SFWs are considered (not shown).

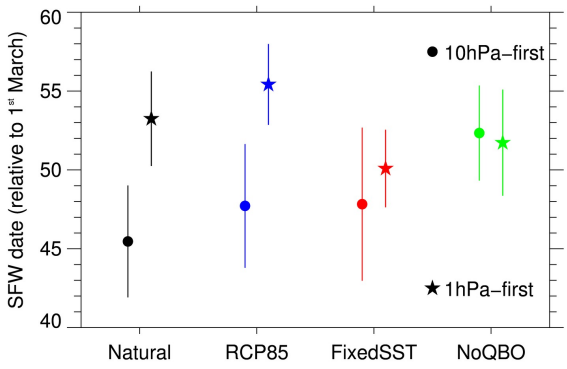

Figure 11. Averaged timing (number of days since the 1st of March) of the (star) 1-hPa first and (dots) 10-hPa first SFWs for the four CESM(WACCM) experiments. Bars indicate the 2-σ confidence intervals.

An additional noticeable feature of the SFWs averaged timing is the anomalously late 1-hPa first SFWs found in the RCP85 experiment (Figure 11), which is consistent with the climatologically stronger polar westerly anomalies found in April (Figure 10c), and which should be related to changes in ODS and/or GHG concentrations. Figure 12 shows the time evolution of the SFW timing (panel a) and the geopotential height (panel b) over the polar cap at 10 hPa in April for the years when a 1-hPa first SFW occurred in the RCP85 experiment. The 1-hPa first SFW timing is not stationary over time. Our results rather suggest that from 1955 to 2010 (2010 to 2099), 1-hPa first SFWs tend to occur increasingly later (earlier) in spring as indicated by the positive (negative) trend of ~3 days (-1.5 days) per decade (Figure 12a). This piecewise SFW timing evolution is consistent with the evolution of the polar vortex strength in April as diagnosed by the geopotential height (Figure 12b) which shows that the spring polar vortex gradually deepens (weakens) before (after) 2010. Note that this piecewise evolution is not found in the Natural, NoQBO and FixedSST experiments (not shown). Furthermore, the inflection period (near 2010) coincides with the onset of the ozone recovery in the Northern Hemisphere in the RCP85 experiment

Commented [u59]: I think according to the setup it has to be related to GHGs or ODS.

Commented [rt60R59]: I changed "may" for "should".

(see Figure 2 of *Lubis et al*. [2016] which shows the ozone recovery in this CESM(WACCM) RCP85 experiment). These results hence suggest that SFW timing may be influenced by ODSs and related to long-term ozone changes.

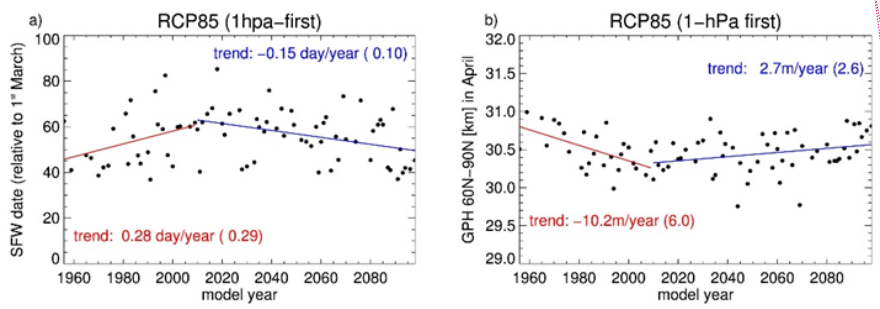

Figure 12. Annual evolution of (a) the 1-hPa first SFWs timing and (b) the April polar cap mean geopotential height for years associated with 1-hPa first SFWs in the RCP85 experiment. Brackets indicate the 2-σ error of the trend estimate.

6 Summary and discussion

This work examines the dynamics, surface signals and drivers of the variability of boreal stratospheric final warmings (SFWs) based on multi-decadal simulations of the CESM(WACCM) and EMAC-O models, and the ERA-Interim dataset. SFWs are classified according to their vertical temporal development [*Hardiman et al*., 2011]: i.e. events can occur first in the mid-stratosphere (10-hPa first SFWs) or in the upper stratosphere (1-hPa first SFWs).

We demonstrate that the CESM(WACCM) and EMAC-O models are able to simulate the two types of SFWs (i.e. 10-hPa and 1-hPa first) identified in reanalyses [*Hardiman et al*., 2011]. However, both models simulate more frequent 1-hPa first SFWs (greater than 50%) than 10-hPa first SFWs (lower than 40%), in contrast to ERA-I that shows a vast majority of 10-hPa first SFWs (55%) against only 21% of 1-hPa first SFWs. We found that the type of SFW is linked to the polar vortex strength in March: 1-hPa/10-hPa first SFWs are preceded by an anomalous strong/weak polar vortex. Given that the climatological polar vortex of both models is anomalously strong in late winter, it is likely that this contributes to the anomalously high frequency of 1-hPa first SFWs in models compared to reanalysis.

In springtime, CESM(WACCM) and EMAC-O simulations reveal a statistically significant surface signal associated with the type of SFW, which projects onto a pattern resembling the AO/NAO as found in *Hardiman et al*. [2011] based on reanalysis data. In the CESM(WACCM) experiments, the NAO-like surface response to SFW variability is further associated with a tripolar sea surface temperature pattern in the North Atlantic sector. Note however that this SST anomaly is not detected in the reanalysis and

Commented [u61]: Is this the right reference for ozone recovery? What about Pazmino et al 2018?

Commented [rt62R61]: In this case, Lubis et al. (2016) is well adapted since they examined the same experiment as we do.

Commented [u63]: I'd be very reluctant with this interpretation. While the figure shows nicely different slopes for the two periods which can only be due to the change from ozone decline to ozone recovery, the trends are hardly significant. What does a trend of -0.15 mean? For which period?
Note that it is one of the statements in the upcoming WMO 2018 ozone assessment that due to the large dynamical variability trends of ozone recovery are not yet detectable in the Arctic.

Commented [BA64R63]: I partially agree with that. It is true that the trend seems to be very small (only 0.15 days/year) and the variability seems to be high. However this trend extends along 9 decades and according to the estimate of error of the trend it seems to be statistically significant.

Commented [rt65R63]: Well, of course it's a bit speculative, but it would be strange not to mention this since it makes sense and the results are significant (although weak). The simulated time period is also quite long compared to the observed period on which attempt of the ozone recovery are currently made and fail in the Arctic. I changed "is" by "may be" (to be more cautious) and added the units of the trends.

Commented [BA66]: Is it not there or is it not statistically significant?

Commented [rt67R66]: Not there; there is no signal.

Commented [u68]: Osso et al 2018 also used ERA-I. So, if the CESM SST anomaly does not show up in ERA-I, the predictability found by Osso must have different reasons.

Commented [rt69R68]: Yes, you're right, the potential link is not direct and may be misleading. I removed the reference to Osso et al. (2018).

the EMAC-O simulation, presumably because the number of years is too short to separate the SFW SST signal from other sources of ocean variability.

Given the potential impact of SFW variability on the seasonal forecast, we then examined whether particular wintertime stratospheric conditions can influence SFWs. Notably, the large amount of model data allowed us to deduce that both SFW types are associated with some characteristics in the occurrence of mid-winter SSWs. Both models reveal that winters with SSWs are more likely to be followed by 10-hPa SFWs, while winters without SSWs usually end with 1-hPa SFWs. Furthermore, if a SSW is recorded in winters preceding 1-hPa first SFWs, the SSW is more likely to occur significantly earlier in the season than for the case of 10-hPa first SFWs. The link between SSW and SFW is only partially reproduced in ERA-I. Although we show that the ERA-I period is too short to allow for deriving a statistically significant relationship between SSW occurrence and SFW types, possible shortcomings in the representation of stratospheric dynamical variability in the two models cannot be discarded.

The separate analysis of the CESM(WACCM) sensitivity experiments revealed that the interannual variability of sea surface temperature and stratospheric equatorial wind has a substantial influence on the type of SFW. We found that removing transient sea surface temperature triggers a climatological stronger polar vortex and a reduced number of SSWs, which in turn leads to a significant increase/decrease of the 1-hPa first/10-hPa first SFW frequency. Conversely, removing the QBO nudging in the tropical stratosphere (leading to relatively constant weak easterlies) induces an increase/decrease of the 10-hPa first/1-hPa first SFW frequency, which is consistent with the increased frequency of SSWs found in January/February (i.e. favoring 10-hPa first occurrence). This further agrees with the findings of *Gray et al*. [2004], based on idealized experiments, that showed that imposing easterlies at any height in the tropical stratosphere increases the frequency of SSWs. A link between the QBO phase and SFW frequency is not clear, however. In CESM(WACCM), we found that 10-hPa first SFWs are associated with equatorial westerly/easterly anomalies centered at 10 hPa/50 hPa and the opposite for 1-hPa SFWs. This appears consistent with the Holton-Tan relationship: i.e. the easterly QBO phase (defined at 50 hPa) leads to a more disturbed polar vortex in winter, and hence to a higher chance of 10-hPa first SFW to occur in spring. Our CESM(WACCM) findings are however neither supported by ERA-I (our study or *Hardiman et al*. [2011]) nor EMAC-O. This suggests a clear model dependency of this relationship, which may be a consequence of the QBO nudging procedure. Further investigation based on experiments with an internally generated QBO would be necessary to test the robustness of the QBO/SFW relationship in CESM(WACCM).

Finally, the sensitivity of SFW characteristics to long-term changes in greenhouse gas and ozone depleting substance concentrations is investigated. While the distribution of SFW frequency appears not to be affected by these changes, their timing does. Namely, 1-hPa first SFWs tend to occur increasingly later/earlier during the ozone depletion/recovery period, which is consistent with trends in the strength

Commented [u70]: Are they imposed? They develop in a model without QBO.

Commented [rt71R70]: Yes thanks for noticing, I revised the text accordingly

of the polar vortex in April. Although the analysis of additional and independent model experiments is required to assess the robustness of this finding, it may provide an additional sign of the impact of ozone changes on Arctic stratosphere dynamical evolution, stressing the importance of accounting for ozone-circulation feedback when simulating long-term stratosphere and climate evolution [*Previdi and Polvani*, 2014].

Overall, this model-based study provides a better understanding of the processes driving the springtime dynamical variability of the boreal stratosphere and its connection with the near-surface climate. As a final remark it is important to highlight that many of our main findings in this study could be determined thanks to the very large dataset offered by the multiple model realizations that allowed to considerably enhanced the signal-to-noise ratio. This would not have been possible by restricting our study to reanalysis data solely.

Commented [u72]: Please see my comment above

Commented [rt73R72]: I'm more careful in the formulation but still maintain that this result is worth noticing.

Commented [u74]: I think it should be mentioned that in your analysis you excluded solar decadal variability as a possible source of SFW variability.
At least the HT mechanism is different for solar max and min, which affects the QBO-SFW link, at least in ERA-I and EMAC-O.

Commented [rt75R74]: I prefer not to mention the solar variability aspect since we did not examine this in the paper.

Commented [BA76]: I would include a final sentence about the relevance of the study. Some characteristics that we could determine of both types of SFWs thanks to the large amount of data that allow us to have a large signal-to-noise ratio.

Commented [rt77R76]: I drafted something in the last paragraph. Please check carefully… I'm not sure of it.

Acknowledgments

This project was supported by the European Project StratoClim (7th framework programme, Grant agreement 603557) and the Grant 'SOLSPEC' from the Centre d'Etude Spatiale (CNES). RT was supported by a grant from the LABEX L-IPSL (ANR-10-LABX-0018), funded by the French Agence Nationale de la Recherche under the 'Programme d'Investissements d'Avenir'. BA was supported by "Ayudas para la contratación de personal postdoctoral en formación en docencia e investigación en departamentos de la Universidad Complutense de Madrid". The CESM(WACCM) simulations were performed at the Deutsche Klimarechenzentrum (DKRZ) Hamburg, Germany. We thank Dr. Steven Hardiman for helpful discussions. Model data and codes used in this study are archived at the GEOMAR's server and are available on request by contacting the corresponding author at remi.thieblemont@latmos.ipsl.fr. The source code of the Community Earth System Model version 1.0 (CESM 1.0) used in this study is publicly distributed and can be obtained after registration at http://www.cesm.ucar.edu/models/cesm1.0/. ERA-Interim data used in this study are available at http://apps.ecmwf.int/datasets/ after registration.

References

Ayarzagüena, B., and E. Serrano (2009), Monthly characterization of the tropospheric circulation over the Euro-Atlantic area in relation with the timing of stratospheric final warming, *J. Climate*, 22, 6313–6324.

Ayarzagüena, B., et al. (2018), No robust evidence of future changes in major stratospheric sudden warmings: A multi-model assessment from CCMI, *Atm. Chem. Phys.*, 18, 11277-11287, https://doi.org/10.5194/acp-18-11277-2018.

Bell, C.J., L.J. Gray, and J. Kettleborough (2010), Changes in the Northern Hemisphere, stratospheric variability under increased CO_2 concentrations, *Q. J. R. Meteorol. Soc.*, 136, 1181-1190.

Black, R.X. and B.A. McDaniel (2007), The Dynamics of Northern Hemisphere Stratospheric Final Warming Events. *J. Atmos. Sci*., 64, 2932–2946, https://doi.org/10.1175/JAS3981.1

Butler, A. H., L. M. Polvani, and C. Deser, (2014), Separating the stratospheric and tropospheric pathways of El Niño–Southern Oscillation teleconnections. *Environ. Res. Lett*., 9, 024014, doi:https://doi.org/10.1088/1748-9326/9/2/024014.

Calvo N., Giorgetta M.A., Peña-Ortiz C. (2007): Sensitivity of the boreal winter circulation in the middle atmosphere to the quasi-biennial oscillation in MAECHAM5 simulations. *Journal of Geophysical Research*, 112, D10124, doi: 10.10296/2006JD007844.

Calvo, N., M. Iza, M.M. Hurwitz, E. Manzini, C. Peña-Ortiz, A.H. Butler, C. Cagnazzo, S. Ineson, and C.I. Garfinkel (2017), Northern Hemisphere Stratospheric Pathway of Different El Niño Flavors in Stratosphere-Resolving CMIP5 Models. *J. Climate*, 30, 4351–4371, https://doi.org/10.1175/JCLI-D-16-0132.1

Camp, C.D., and K.K. Tung (2007), The influence of the solar cycle and QBO on the late winter stratospheric polar vortex, *J. Atmos. Sci*., 64, 1267-1283.

Czaja, A., and C. Frankignoul (2002), Observed impact of Atlantic SST anomalies on the North Atlantic Oscillation, *J. Climate*, 15, 606-623.

Dee, D. P., et al. (2011), The ERA-Interim reanalyses: configuration and performance of the data assimilation system, *Q. J. R. Meteorol. Soc.*, 137, 553–597, doi:10.1002/qj.828.

Garfinkel, C.I., and D.L. Hartmann (2008), Different ENSO Teleconnections and Their Effects on the Stratospheric Polar Vortex, *J. Geophys. Res. Atmos*, 113, D18114, doi:10.1029/2008JD009920.

Gent, P. R., et al. (2011), The Community Climate System Model Version 4, *J. Clim.*, 24(19), 4973–4991, doi:10.1175/2011JCLI4083.1.

Gray, L. J., S. J. Phipps, T. J. Dunkerton, M. P. Baldwin, E. F. Drysdale, and M. R. Allen (2001), A data study of the influence of the equatorial upper stratosphere on Northern Hemisphere stratospheric sudden warmings, *Q. J. R. Meteorol. Soc*., 127, 1985–2003.

Gray, L. J., S. Crooks, C. Pascoe, S. Sparrow, and M. Palmer (2004), Solar and QBO Influences on the timing of stratospheric sudden warmings, *J. Atmos. Sci*., 61, 2777–2796.

Hansen, F., Matthes, K. and Gray, L.J. (2013), Sensitivity of stratospheric dynamics and chemistry to QBO nudging width in the chemistry-climate model WACCM, *J. Geophys. Res.- Atmos*., 118 (18), pp. 10464-10474. DOI.10.1002/jgrd.50812.

Hansen, F., Matthes, K., Petrick, C. and Wang, W. (2014) The influence of natural and anthropogenic factors on major stratospheric sudden warmings, *J. Geophys. Res.- Atmos.*, 119 (13). pp. 8117-8136. DOI 10.1002/2013JD021397.

Hardiman, S. C., et al. (2011), Improved predictability of the troposphere using stratospheric final warmings, *J. Geophys. Res.*, 116, D18113, doi:10.1029/2011JD015914.

Holton, J.R., and H.-C. Tan (1980), The influence of the equatorial quasi-biennial oscillation on the global circulation at 50 mb, *J. Atmos. Sci.*, 37, 2200-2208.

Hu, J., R. Ren, and H. Xu (2014), Occurrence of Winter Stratospheric Sudden Warming Events and the Seasonal Timing of Spring Stratospheric Final Warming. *J. Atmos. Sci*., 71, 2319–2334, https://doi.org/10.1175/JAS-D-13-0349.1

Hurwitz, M. M., P. A. Newman, and C. I. Garfinkel (2012), On the influence of North Pacific sea surface temperature on the Arctic winter climate, *J. Geophys. Res*., 117, D19110, doi:10.1029/2012JD017819.

Jöckel, P., H. Tost, A. Pozzer, C. Brühl, J. Buchholz, L. Ganzeveld, P. Hoor, A. Kerkweg, M. G. Lawrence, R. Sander, B. Steil, G. Stiller, M. Tanarhte, D. Taraborelli, J. Van Aardenne, J. Lelieveld (2006), The atmospheric chemistry general circulation model ECHAM5/MESSy: consistent simulation of ozone from the surface to the mesosphere. *Atmos Chem Phys,* 6, 5067–5104.

Jungclaus, J. H., N. Keenlyside, M. Botzet, H. Haak, J. J. Luo, M. Latif, J. Marotzke, U. Mikolajewicz, E. Roeckner (2006), Ocean circulation and tropical variability in the coupled model ECHAM5/MPI-OM. *J Clim*., 19, 3952–3972.

Kim, J., S.-W. Son, E.P. Gerber, and H.-S. Park (2017), Defining sudden stratospheric warming in climate models: Accounting for biases in model climatologies, *J. Climate*, 30, 5529-5546.

Kinnison, D. E., et al., 2007, Sensitivity of chemical tracers to meteorological parameters in the MOZART-3 chemical transport model. *J. Geophys. Res*., 112, D20302, doi:https://doi.org/10.1029/2006JD007879

Labitzke, K. (1981), Stratospheric-mesospheric midwinter disturbances: A summary of observed characteristics, *J. Geophys. Res.*, 86, C10, 9665–9678.

Lean, J. L., G. Rottman, J. Harder, and G. Kopp (2005), Source contributions to new understanding of global change and solar variability. *Sol. Phys.*, **230**, 27–53, doi:10.1007/s11207-005-1527-2.

Lubis, S.W., N. Omrani, K. Matthes, and S. Wahl (2016), Impact of the Antarctic Ozone Hole on the Vertical Coupling of the Stratosphere-Mesosphere-Lower Thermosphere System. *J. Atmos. Sci*., 73, 2509–2528, https://doi.org/10.1175/JAS-D-15-0189.1

Manney, G. L., N. J. Livesey, C. J. Jimenez, H. C. Pumphrey, M. L. Santee, I. A. MacKenzie, and J. W. Waters (2006a), EOS Microwave Limb Sounder observations of "frozen-in" anticyclonic air in Arctic summer, *Geophys. Res. Let.*, Vol. 33, L06810, doi:10.1029/2005GL025418.

Manney, G.L., M.L. Santee, L.Froidevaux, K. Hoppel, N.J. Livesey , and J.W.Waters (2006b), EOS MLS observations of ozone loss in the 2004-2005 Arctic winter, *Geophys.Res.Lett*., 33, L04802, doi:10.1029/2005GL024494.

Manney, G., et al. (2011), Unprecedented Arctic ozone loss in 2011, *Nature*, 478, 469–475.

Manney, G.L., and Z.D. Lawrence (2016), The major stratospheric final warming in 2016: dispersal of vortex air and termination of Arctic chemical ozone loss, *Atmos Chem Phys.*, 16, 15371-15396, https://doi.org/10.5194/acp-16-15371-2016.

Marsh, D., M. J. Mills, D. E. Kinnison, J.-F. Lamarque, N. Calvo, and L. M. Polvani (2013), Climate change from 1850 to 2005 simulated in CESM1(WACCM), *J. Clim.*, 26, 7372–7391, doi:10.1175/JCLI-D-12-00558.1.

Matthes, K., D. R. Marsh, R. R. Garcia, D. E. Kinnison, F. Sassi, and S. Walters (2010), Role of the QBO in modulating the influence of the 11 year solar cycle on the atmosphere using constant forcings, *J. Geophys. Res.*, 115, D18110, doi:10.1029/2009JD013020.

Matthes, K., K. Kodera, R.R. Garcia, Y. Kuroda, D.R. Marsh, and K. Labitzke (2013), The importance of time-varying forcing for QBO modulation of the atmospheric 11 year solar cycle signal, *J. Geophys. Res.*, 118, 4435-4447, doi:10.1002/jgrd.50424.

Meinshausen, M., et al. (2011), The RCP greenhouse gas concentrations and their extensions from 1765 to 2300, *Clim. Change*, 109(1–2), 213–241, doi:10.1007/s10584-011-0156-z.

Mitchell, D.M., S. Osprey, L.J. Gray, N. Butchart, S.C. Hardiman, A.J., Charlton-Perez and P. Watson (2012), The effect of climate change on the variability of the Northern Hemisphere stratospheric polar vortex, *J. Atmos. Sci*., 69, 2608-2618.

Mlynczak, M. G., C. J. Mertens, R. R. Garcia, and R. W. Portmann (1999, A detailed evaluation of the stratospheric heat budget: 2. Global radiation balance and diabatic circulations. J. Geophys. Res., 104, 6039–6066, https://doi.org/10.1029/1998JD200099.

Mudelsee, M. (2014), Climate Time Series Analysis: Classical Statistical and Bootstrap Methods. 717 Second edition. Springer, Cham Heidelberg New York Dordrecht London.

Previdi, M., and L. M. Polvani (2014), Climate system response to stratospheric ozone depletion and recovery, *Q. J. R. Meteorol. Soc*., 140, 2401–2419, doi:10.1002/qj.2330.

Naujokat, B. (1986), An update of the observed quasi-biennial oscillation of the stratospheric winds over the tropics, *J. Atmos. Sci*., 43, 1873–1877.

Omrani, N.-E., N. Keenlyside, J. Bader, and E. Manzini (2014), Stratosphere key for wintertime atmospheric response to warm Atlantic decadal conditions, *Climate Dyn*., 42, 649–663, doi:https://doi.org/10.1007/s00382-013-1860-3.

Salby, M. L., and P. F. Callaghan (2007), Influence of planetary wave activity on the stratospheric final warming and spring ozone, *J. Geophys. Res*., 112, D20111, doi:10.1029/2006JD00753

SPARC CCMVal (2010), SPARC Report on the Evaluation of Chemistry-Climate Models, V. Eyring, T. G. Shepherd, D. W. Waugh (Eds.), *SPARC Report No. 5*, WCRP-132, WMO/TD-No. 1526.

Thiéblemont, R., N. Huret, Y. J. Orsolini, A. Hauchecorne, and M.-A. Drouin (2011), Frozen-in anticyclones occurrinsg in polar Northern Hemisphere during springtime: Characterization, occurrence and link with quasi-biennial oscillation, *J. Geophys. Res.*, 116, D20110, doi:10.1029/2011JD016042.

Thiéblemont, R., Y. J. Orsolini, A. Hauchecorne, M.-A. Drouin, and N. Huret (2013), A climatology of frozen-in anticyclones in the spring arctic stratosphere over the period 1960–2011, *J. Geophys. Res. Atmos.*, 118, 1299–1311, doi:10.1002/jgrd.50156.

Visbeck, M., Chassignet, E., Curry, R., Delworth, T., Dickson, B. & Krahmann, G. (2003), The ocean's response to North Atlantic oscillation variability, in *The North Atlantic Oscillation*, edited by J. Hurrell, Y. Kushnir, G. Ottersen, and M. Visbeck, American Geophysical Union monograph.

Watson, P.A. and L.J. Gray (2014), How Does the Quasi-Biennial Oscillation Affect the Stratospheric Polar Vortex?. *J. Atmos. Sci*., 71, 391–409, https://doi.org/10.1175/JAS-D-13-096.1

Waugh, D.W., Randel, W.J., Pawson, S., Newman, P.A., and Nash, E.R. (1999), Persistence of the Lower Stratospheric Polar Vortices. *J. Geophys. Res* , 104, 27191-27201.

Waugh, D. W., and P. P. Rong (2002), Interannual variability in the decay of lower stratospheric Arctic vortices, *J. Meteorol. Soc. Jpn.*, 80, 997–1012.

Wei, K., W. Chen, and R. H. Huang (2007), Dynamical diagnosis of the breakup of the stratospheric polar vortex in the Northern Hemisphere, *Sci. China Ser. D*, 50 (9), 1369–1379, doi:10.1007/s11430-007-0100-2